Changes in climate and land use have a larger direct impact than rising CO_2 on global river runoff trends

Shilong Piao*, Pierre Friedlingstein*†, Philippe Ciais*, Nathalie de Noblet-Ducoudré*, David Labat‡, and Sönke Zaehle*

*Institut Pierre Simon Laplace, Laboratoire des Sciences du Climat et de l'Environnement, Commissariat à l'Énergie Atomique, 91191 Gif sur Yvette, France; and ‡Laboratoire de Mécanisme de Transfert en Géologie, Unité Mixte de Recherche 5563, Centre National de la Recherche Scientifique/Institut de Recherche pour le Développement/Université de Paris Sud 14, Avenue Edouard Belin, 31400 Toulouse, France

Communicated by Inez Y. Fung, University of California, Berkeley, CA, August 3, 2007 (received for review October 25, 2006)

The significant worldwide increase in observed river runoff has been tentatively attributed to the stomatal "antitranspirant" response of plants to rising atmospheric CO_2 [Gedney N, Cox PM, Betts RA, Boucher O, Huntingford C, Stott PA (2006) *Nature* 439: 835–838]. However, CO_2 also is a plant fertilizer. When allowing for the increase in foliage area that results from increasing atmospheric CO_2 levels in a global vegetation model, we find a decrease in global runoff from 1901 to 1999. This finding highlights the importance of vegetation structure feedback on the water balance of the land surface. Therefore, the elevated atmospheric CO_2 concentration does not explain the estimated increase in global runoff over the last century. In contrast, we find that changes in mean climate, as well as its variability, do contribute to the global runoff increase. Using historic land-use data, we show that land-use change plays an additional important role in controlling regional runoff values, particularly in the tropics. Land-use change has been strongest in tropical regions, and its contribution is substantially larger than that of climate change. On average, land-use change has increased global runoff by 0.08 mm/year^2 and accounts for ≈50% of the reconstructed global runoff trend over the last century. Therefore, we emphasize the importance of land-cover change in forecasting future freshwater availability and climate.

atmospheric CO_2 | water cycle | climate change | land cover change

Climate change and human intervention are expected to strongly alter the global hydrological cycle in the coming decades (1–5). Previous reconstruction of global runoff data suggests that global river runoff increased significantly during the 20th century (2). However, it is difficult to estimate whether this trend in runoff is caused by natural or anthropogenic factors, because the characteristics and dynamic properties of the hydrological cycle depend on many interrelated links among climate, atmosphere, soil, and vegetation dynamics. Long-term changes in runoff depend on the balance of precipitation and evapotranspiration. The latter term is not only driven by climatic factors, such as temperature, wind speed, surface humidity, and solar radiation, but also is modulated by physiological (e.g., stomatal) and structural [e.g., leaf area index (LAI)] components of vegetation. It is well known that stomata respond to elevated atmospheric CO_2 concentrations by partial closure (6). Accordingly, a recent modeling analysis suggested that the rising atmospheric CO_2 concentration is the main driver of the observed increase in continental runoff (1). Nevertheless, the results of the Gedney *et al.* (1) study should be viewed with caution because only the direct effect of atmospheric CO_2 concentrations on stomatal conductance was considered. Structural changes in vegetation in response to increased productivity under higher atmospheric CO_2 levels, particularly changes in LAI (7), were not taken into account in their study.

Land use is another key factor controlling the water balance of ecosystems and the associated river runoff. Land use changes already impacted the terrestrial water cycle and will continue to do so in the next century (8–11). However, globally comprehensive analyses of the impacts of land-use change on runoff are scarce, especially compared with studies relating the effects of land-use change on the global carbon cycle. Here we investigate how historical changes in cropland establishment and abandonment, combined with atmospheric CO_2 and climate change, have modified the regional and global runoff patterns. We used a process-based terrestrial biosphere model, organizing carbon and hydrology in dynamics ecosystems (ORCHIDEE) (12), to separately quantify the hydrological contribution of the driving factors.

Results

ORCHIDEE-derived global total runoff because of changes in atmospheric CO_2, climate, and land use (simulation E3) is $41.4 \pm 3.1 \times 10^{12}$ m^3/year (given our resolution that the surface global area is 137.6×10^6 km^2). This figure corresponds to an average global runoff that varies between 267 and 339 mm/year^{-1}, with a mean value of 301 mm/year for 1901 to 1999. This value agrees well with the current observed range of 35.2 to 45.1×10^{12} m^3/year (2, 13). The modeled decadal variability of global runoff in simulation E3 is consistent with the reconstructed global runoff data, which account for 221 discharge time series available at the mouth of the main rivers of the world (2) ($R = 0.68$, $P < 0.001$) (Fig. 1*A*). On average, the modeled global mean runoff due to the combined effects of climate, land use, and atmospheric CO_2 (simulation E3) reveals a significant positive trend of 0.17 mm/year^2 ($R = 0.31$, $P = 0.002$), which is close to the observation-based trend of 0.18 mm/year^2 (2).

Long-term runoff changes result from the balance of precipitation and evapotranspiration. Climate observations indicate that annual precipitation significantly increased by ≈0.2 mm/year^2 ($P < 0.001$) in the last century. Simulated evapotranpiration associated with climate change (simulations E2–E1) shows an upward trend of ≈0.07 mm/year^2 ($P < 0.001$). As a result, the runoff change, driven by climate trends and variability alone, is ≈0.13 mm/year^2 (simulations E2–E1) and, hence, is not sufficient to account for the entire modeled trend in global runoff (simulation E3) (Fig. 1*B* and Table 1).

The atmospheric CO_2 concentration interacts with the hydrological cycle in two main ways: reducing transpiration per unit of leaf area and increasing productivity per unit of leaf area, eventually leading to changes in plant structure and an increased foliage area (7, 14). A significant increase in global runoff during

Author contributions: S.P., P.F., and P.C. designed research; S.P., P.F., P.C., N.d.N.-D., D.L., and S.Z. performed research; S.P., P.F., and P.C. analyzed data; and S.P., P.F., P.C., N.d.N.-D., D.L., and S.Z. wrote the paper.

The authors declare no conflict of interest.

Freely available online through the PNAS open access option.

Abbreviations: LAI, leaf area index; ORCHIDEE, organizing carbon and hydrology in dynamics ecosystems; PT, plant transpiration.

†To whom correspondence should be addressed. E-mail: pierre.friedlingstein@lsce.ipsl.fr.

This article contains supporting information online at www.pnas.org/cgi/content/full/0707213104/DC1.

© 2007 by The National Academy of Sciences of the USA

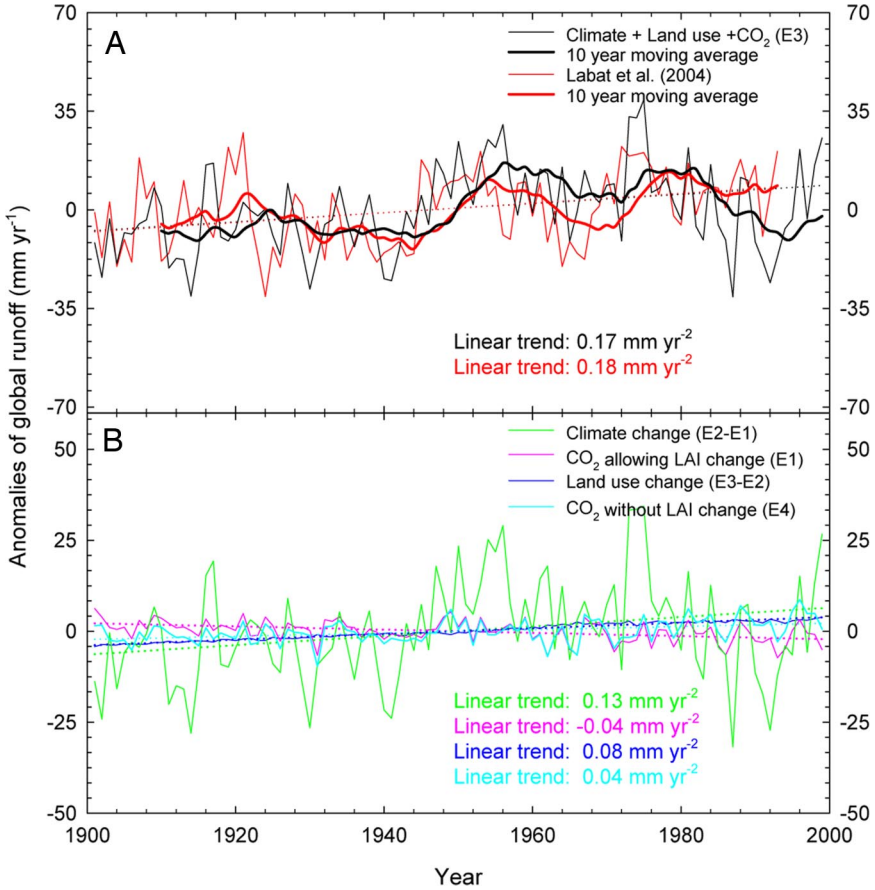

Fig. 1. Change in global runoff anomalies from 1901 to 1999. (*A*) Comparison of global runoff change between that reconstucted by Labat *et al.* (2) and that modeled in simulation E3, including climate, atmospheric CO_2, and land-use change. (*B*) Interannual variation and trend in modeled global runoff resulting from the effects of increased atmospheric CO_2 (simulation E1), climate change (simulations E2–E1), land-use change (simulations E3–E2), and a decrease in stomatal conductance associated with rising atmospheric CO_2 (simulation E4), respectively. The ORCHIDEE-simulated global runoff in simulation E3 shows a significant increasing trend with a rate of 0.17 mm/year^2 during the last century, which is close to the estimation of 0.18 mm/year^2 by Labat *et al.* (2). The global runoff trend derived from simulation E4 is estimated to be ≈0.16 mm/year^2 for the period from 1960 to 1999, which is close to the study of Gedney *et al.* (1), who estimated a trend of ≈0.2 mm/year^2 in response to the reduced leaf-level stomatal conductance because of rising atmospheric CO_2 since 1960.

the last century (0.04 mm/year^2; $P < 0.001$) was predicted when only the response of canopy conductance to rising atmospheric CO_2 was considered and when the effect of plant structure changes was ignored (simulation E4) (Fig. 1*B*). From 1960 to 1999, the antitranspirant effect was estimated to be ≈0.16 mm/year^2 (simulation E4), which is close to the study of Gedney *et al.* (1), who estimated a trend of ≈0.2 mm/year^2 in response to the reduced leaf-level stomatal conductance because of rising atmospheric CO_2 since 1960. Allowing for the changes in LAI that result from elevated CO_2 concentration (simulation E1), we predicted a slight but significant decline in global runoff of 0.04 mm/year^2 ($P < 0.001$) associated with the rise in atmospheric CO_2 of 70 ppm per volume (ppmv) from 1901 to 1999 (Fig. 1*B*). This result indicates that the net effect of increased vegetation LAI in response to CO_2 (+10%) provides a greater cumulative surface area for canopy water transpiration and interception and enhances evapotranspiration by ≈0.08 mm/year^2 (simulations E1–E4). In other words, the net effect of rising atmospheric CO_2 on modeled transpiration is positive and in overall agreement with independent results from coupled modeling studies of climate–vegetation interactions (15, 16). Our results do not support the view of Gedney *et al.* (1), which is that elevated CO_2 was the primary contributor to the increase in global runoff during the last century. Global mean evapotranspiration per leaf area (the ratio of evapotranspiration to LAI) generated from simulation E1 clearly decreased by ≈9% during the last century ($P < 0.001$).

Land-use changes caused a marked increase in global runoff by ≈0.08 mm/year^2 from 1901 to 1999 (simulations E3–E2) (Fig. 1*B*). This land-use-related trend was mainly the result of defor-

Table 1. Observed and ORCHIDEE-modeled global runoff trends (mm/year^2) over the 20th century

Trends	CO_2 (simulation E1)	CO_2 + climate (simulation E2)	CO_2 + climate + land use (simulation E3)	Labat *et al.* (2)	Gedney *et al.* (1)
Global trends	−0.04	0.09	0.17	0.18	0.19

The Gedney *et al.* (1) study trend (simulation ALL) also is given for comparison.

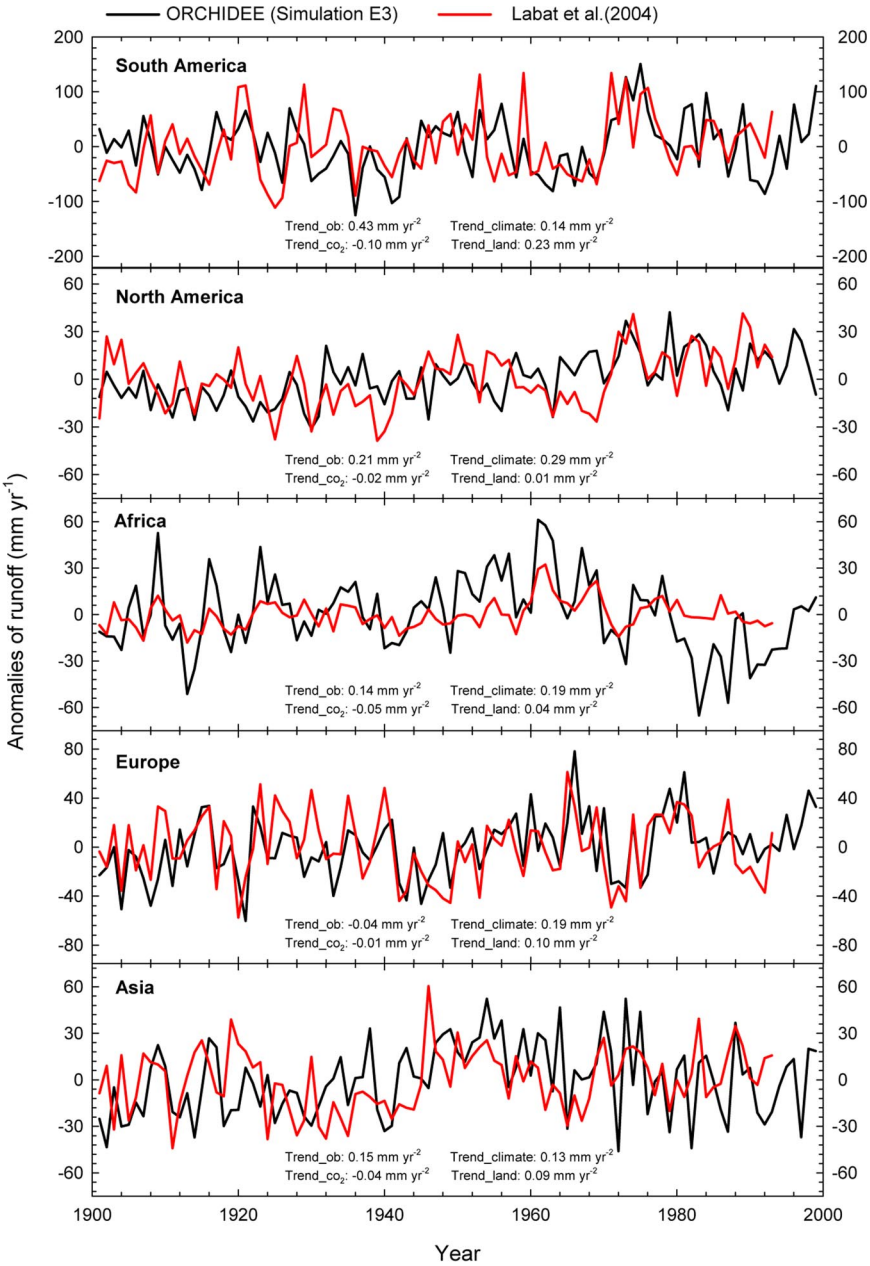

Fig. 2. Change in the runoff anomalies during the 20th century in the different continental regions. All continents show that the runoff derived from simulation E3 is significantly correlated with that estimated by Labat *et al.* (2) ($P < 0.02$). Because of the small number (seven) of observing stations that were available in Africa since 1983, the trend in Africa runoff is calculated based on the period from 1901 to 1982. Trend_ob, runoff trend reconstructed by Labat *et al.* (*2*); Trend_climate, the modeled runoff trend because of climate change (simulations E2–E1); Trend_CO_2, the modeled runoff trend because of increasing atmospheric CO_2 (allowing LAI changes) (simulation E1); Trend_land, the modeled runoff trend because of land use change (simulations E3–E2). The sum of Trend_climate, Trend_CO_2, and Trend_land reflects the runoff trend derived from simulation E3 that consider all factors change.

estation. On the basis of >600 field observations, Jackson *et al.* (10) reported that tree plantations decreased stream flow by 227 mm/year globally. By applying this ratio to an annual forest clearing rate for croplands of 0.058×10^6 km^2/year, one can predict a rough-and-ready estimated increase of 0.095 mm/year^2 in global runoff because of deforestation, which is close to our estimation (simulations E3–E2). According to our simulations, land-use change accounted for ≈50–55% of the global increase because of all combined environmental changes (simulation E3).

The general agreement between the model results from simulation E3 and observation-based estimates by Labat *et al.* (2) is seen at the global and continental scales (Fig. 2). This result suggests a potential applicability of the model for exploring spatial patterns of runoff change. However, the modeled interannual runoff variability (simulation E3) in Africa was not consistent with that reconstructed by Labat *et al.* (2) since 1983 probably because of the limited number of observing stations (seven) during this period (2). Fig. 3 shows the spatial distribution of trends in runoff, rainfall, and the surface fractional area of croplands during the 20th century. Despite an overall significant increase, the runoff distribution in simulation E3 shows regionally heterogeneous trends (Fig. 3*A*), reflecting the spatial patterns of changes in land use and climatic conditions (Fig. 3 *C* and *D*), chiefly precipitation (Fig. 3*E*). The largest increase in

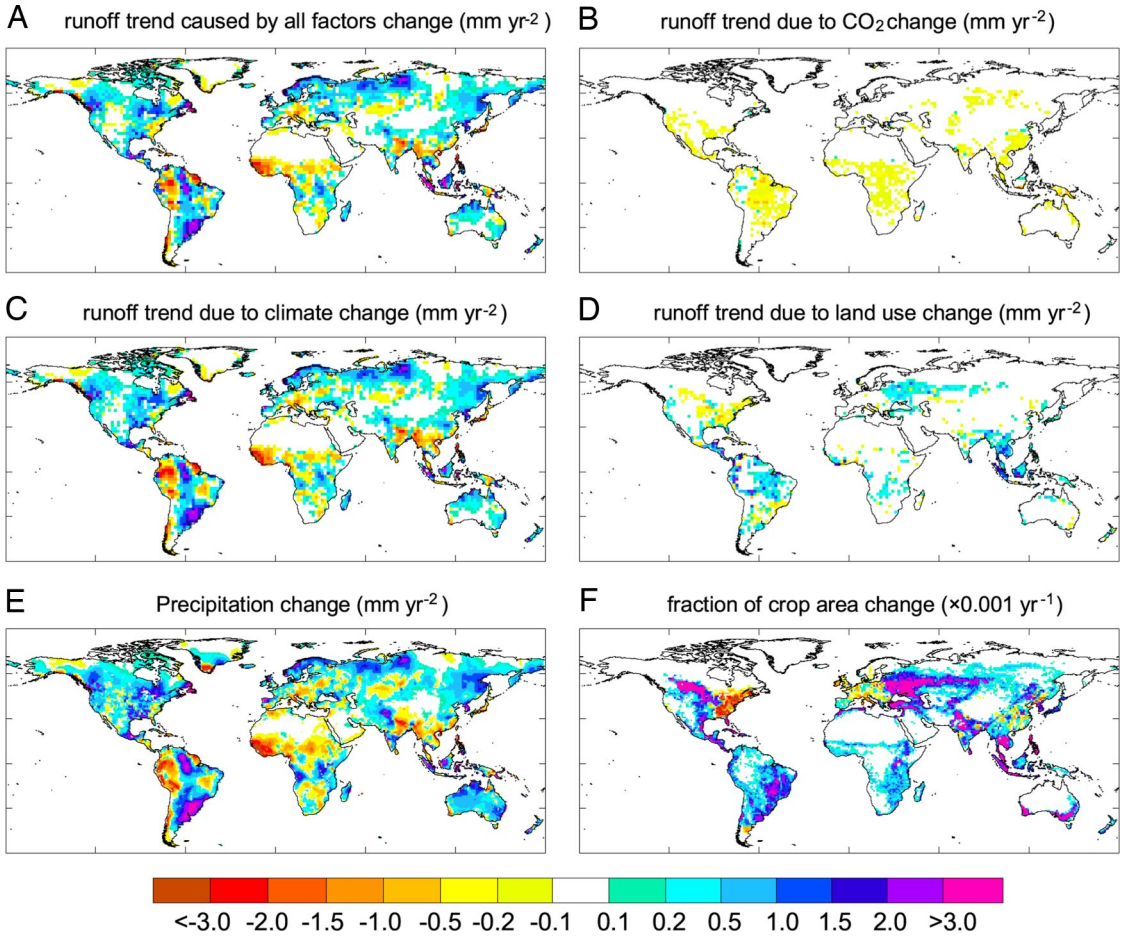

Fig. 3. Spatial distribution of the trend in modeled runoff (*A–D*), precipitation (*E*), and fraction of agriculture area (*F*) over the last century. (*A–D*) Runoff trend because of the combined effects of climate, land use, and atmospheric CO_2 (simulation E3) (*A*); increase in atmospheric CO_2 (allowing LAI changes) (simulation E1) (*B*); climate change (simulations E2–E1) (*C*); and land use change (simulation E3-E2) (*D*).

runoff (>1.0 mm/year^2) was located in the La Plata basin of South America, the eastern part of the Amazon basin, the southeastern quadrant of Africa, eastern Canada, northern Asia, and Indonesia and Malaysia (Fig. 3*A*), where pronounced increases in annual precipitation were observed (Fig. 3*E*). In contrast, as a result of a substantial rainfall deficit (Fig. 3*E*), the western Amazonian region, subSaharan Africa, southern China, and southern Europe all exhibited a strong downward trend in runoff (Fig. 3*A*). Similar spatial patterns of runoff changes also were observed from the runoff observation data compiled by Milly *et al.* (3), except in northern Europe, where significant decreases in runoff were observed. This finding may drive the overestimation of the increase in runoff for Europe (Fig. 2). In accordance with our simulation results (E3), the 20C3M simulations also produced dramatic increases in runoff in northern Europe (3), implying that the observed decrease in runoff for this region may not be related to current climate and land-use changes.

The expansion of croplands (>0.1%/year^1) across southern Asia, eastern Europe, and eastern South America produced a remarkable increase in runoff (>0.2 mm/year^2) over the last century (Fig. 3*D*). In Indonesia and Malaysia, Central America, and northern South America, the contribution of forest clearing to runoff change was larger than the effect of climate change and climatic variations [supporting information (SI) Table 2]. A previous study also found that, although precipitation in the Tocantins Basin of the Amazonian region did not significantly change over the past 40 years, runoff increased by 24%, coincident with the local expansion of agriculture (17). Only a few regions of the globe, principally in eastern North America, displayed a decrease in crop area over the second half of the 20th century (Fig. 3*F*). Consequently, negative trends in runoff are predicted over this region (Fig. 3*A*).

Discussion

A decline in runoff in response to rising atmospheric CO_2 (simulation E1) (Fig. 3*B*) implies a concurrent increase in plant transpiration (PT). Without considering any effects on leaf energy balance, the ecosystem transpiration change between today's CO_2 levels and preindustrial CO_2 levels can be expressed as a function of changes in LAI and in stomatal conductance: $PT(CO_2) = PT_0 \times [1 + \Delta LAI(CO_2)] \times [1 - \Delta S(CO_2)]$, where $PT(CO_2)$ is the value of PT under current CO_2 levels, PT_0 is the preindustrial value of the transpiration, and $\Delta LAI(CO_2)$ and $\Delta S(CO_2)$ are the relative changes in LAI and stomatal conductance, respectively, caused by rising CO_2. This simplified equation assumes a linear relationship between transpiration per leaf area and stomatal conductance. If the term $[1 + \Delta LAI(CO_2)] \times [1 - \Delta S(CO_2)]$ is >1, an increase in transpiration is predicted. On average, an increase in vegetation productivity of 0.13–0.2% per ppm increase in CO_2 (14, 18) and a decreasing stomatal conductance of 0.07% per ppm increase in CO_2 (6) suggest potential increases in transpiration of ≈0.06–0.1% per ppm with rising CO_2, which is comparable with the value of 0.04% per ppm

derived in simulation E1. Notwithstanding, projections of future behavior must be carried out with caution because the response of vegetation growth to elevated CO_2 is a nonlinear process (19). Controlled experiments with plants growing in CO_2-rich environments have indeed indicated that LAI increased sharply from low (200 ppm) to ambient (360 ppm) levels of CO_2 but tended to saturate at higher CO_2 levels (7). As a consequence, it is possible that the continuous increase in atmospheric CO_2 will probably lead to a decline in transpiration in the future, as suggested by field experiments (20).

If there is a decrease in runoff and an increase in PT in response to rising CO_2, such as that suggested by our model simulation E1, then these results have important implications for both soil-water storage and plant growth. During the last century, global soil moisture estimated by simulation E1 declined by $\approx$1% because of elevated CO_2. Such a decrease in soil moisture can exert negative feedbacks on vegetation growth, especially in water-stressed ecosystems. To illustrate the interactions between CO_2-related hydrological changes and vegetation growth, we analyzed the seasonal trends in LAI [monthly values of ΔLAI(CO_2)] and soil-moisture contents for temperate grassland ecosystems (25–50°N) during the last century from simulation E1. The increase in LAI was less pronounced at the end of the growing season than during the early growing season, which is in agreement with the results from FACE experiments (21). Pinter *et al.* (21) found that elevated CO_2 only led to an increase in LAI in the early and middle parts of the growing season. Such a decrease in the response of plant growth to CO_2 was probably associated with fall soil moisture deficits because of prior enhanced vegetation growth. The largest decrease in modeled soil moisture occurred at the end of growing season.

Uncertainties still exist regarding the global runoff trend over the last century, despite the good agreement between the results of simulation E3 (considering the joint effects of atmospheric CO_2, climate, and land-use change) and the observation-based reconstruction of global runoff change (2). For example, agricultural irrigation plays an important role in the global water cycle, particularly in North America and Eurasia (22, 23), but we have too little knowledge about its potential contribution to the runoff trend on a global scale. Because of the lack of information about historical changes in the agriculture irrigation area and water use for irrigation, we did not consider the effects of changes in irrigation on the global runoff trend. A previous study suggested that irrigation diverts water from runoff to evapotranspiration by the order of 4–5% of annual global runoff (24). Therefore, our simulated historical global runoff trend may be overestimated. However, it also is possible that the negative effect of irrigation on runoff is partly compensated for by an increase in precipitation resulting from irrigation-driven enhancements of evapotranspiration (5, 25). Because the comparison with Labat *et al.* (2) is performed at the continental scale, the impact of irrigation on the runoff trend should be relatively small. Further studies based on spatially and temporally explicit historic irrigation data sets are needed to quantify the role that irrigation change plays in the regional and global hydrological cycles.

Conclusions

Process-based simulations of global runoff using a terrestrial biosphere model suggest that the observed significant increase in global runoff in the 20th century was mainly a consequence of climate change and widespread deforestation. We estimate that the secular rise in atmospheric CO_2 caused a small but significant decrease in global runoff because of the antagonistic responses of leaf-level processes and vegetation dynamics. On the basis of our findings, it seems overoptimistic to assume that rising CO_2 could cause water savings in soil and thereby further promote vegetation productivity at a scale large enough to affect continental runoff. The results presented here not only provide insights for large-scale field experiments but also highlight the importance of biosphere feedbacks on the water balance of land surfaces (15, 16). The roles of vegetation growth feedbacks and land-use change cannot be ignored when projecting future changes in hydrologic processes and climate.

Methods

The ORCHIDEE model is a process-based biogeography–biogeochemistry model developed to assess the transient impacts of climate change on the transfer of water and carbon in the vegetation–soil–atmosphere system (12). The model includes parameterizations of canopy physiological processes (photosynthesis and canopy conductance) that are intimately linked to biospheric energy and hydrological balances and operated at a time scale of 30 min. Soil hydrology are modeled as described by Ducoudre *et al.* (26) following a semiempirical approach. There are two soil layers, and the total depth of soil considered at all land points is the root zone. The water content of each layer is updated by accounting for inputs from rainfall, which is reduced by interception losses and snowmelt, as well as by losses to soil evaporation, transpiration, deep drainage, and surface runoff. The amount of water intercepted by the foliage is controlled by the incident rainfall and LAI, and it gives rise to interception losses that depended on the prevailing meteorological conditions. Soil evaporation is calculated from the relative humidity of the air at the land surface and aerodynamic and soil resistances, where the soil resistance was a function of soil moisture. Vegetation transpiration depends on the modeled photosynthetic activity and atmospheric vapor-pressure deficit, as described by Ball *et al.* (27), and is mediated by soil-water availability. Surface runoff and drainage are calculated as the excess water above field capacity in both soil layers.

Vegetation productivity is calculated based on a coupled photosynthesis–water balance scheme. Plant growth based on the net plant carbon gain is allocated to six tissue pools (leaf, root, and wood, as well as reserve and reproductive organs), with a response of the relative investment into above- and belowground structures, depending on soil temperature and moisture. Therefore, the ecosystem water balance affected plant carbon gain and structure. Leaf phenology and decomposition of litter and soil organic matter depend on temperature and water stress. Therefore, modeled water evapotranspiration is an integrator of meteorological, hydrological, and ecological processes. More detailed descriptions of the various components of ORCHIDEE can be found in Krinner *et al.* (12) and Ducoudre *et al.* (26).

The ORCHIDEE model has been widely used to assess the transient impacts of climate change on the global or regional water and carbon cycles (28–32). The seasonal cycles of energy and water exchanges and carbon fluxes from the ORCHIDEE model have been extensively calibrated and validated against eddy covariance data from a number of field sites (12, 33). The global distribution of LAI and runoff (12) and satellite-derived interannual variability in LAI over the recent period are also realistically represented (31, 32).

The monthly climate data sets (temperature, precipitation, wet-day frequency, diurnal temperature range, cloud cover, relative air humidity, and wind speed), with a spatial resolution of 0.5° for 1901–1999, were provided by the Climatic Research Unit (School of Environmental Sciences, University of East Anglia, U.K.) (34). The historical changes in atmospheric CO_2 concentration were taken from Rayner *et al.* (35). Cropland area is prescribed each year from Ramankutty and Foley (36). We combined this data set with that of Goldewijk (37) to account for the extent of pasture. The distribution of natural vegetation at each grid cell is derived from Loveland *et al.* (38). The extent of natural vegetation varied with time as a function of the prescribed extent of cropland and pasture.

Using average climate data from 1901 to 1910, the atmospheric CO_2 concentration, and land cover of 1860, we first ran the model at a 2° resolution until the vegetation and soil carbon pools reached equilibrium. On the basis of this equilibrium status, four simulations from January 1860 to December 1999 were carried out to investigate the relative contribution of atmospheric CO_2, climate change, and land-use change on the global runoff trends and patterns. Because of the lack of climate data before 1901, the average monthly climatology from 1901 to 1910 was used for the 1860–1900 run and for monthly climate data for individual years thereafter.

In simulation E1, atmospheric CO_2 concentration alone was varied. In simulation E2, atmospheric CO_2 and climate were varied. In simulation E3, atmospheric CO_2 concentration, climate, and land use were varied. Finally, we performed an additional simulation (E4), comparable to the one carried out by Gedney *et al.* (1), which only considered the response of stomatal conductance to rising atmospheric CO_2 and did not consider the subsequent effects on vegetation structure, notably the foliage cover. The changes in vegetation growth accompanied by environmental change were taken into account in simulations E1, E2, and E3 to comprehensively evaluate the hydrological contribution of different factors. The individual effects of climate variations were derived as the difference between simulations E2 and E1, and the effects of land use change were estimated by subtracting E2 from E3. The difference of runoff trend between simulations E1 and E4 reflected the effects of LAI changes in response to increased CO_2.

We thank N. Viovy, A. Friend, and R. Alkama for helpful comments and discussions; Cecilia Garrec and Alessandro Tagliabue for English revision; Jean-Yves Peterschmitt, who helped N.d.N.-D. to assemble the crop, pasture, and natural vegetation maps used in this study; and I. Fung, P. C. D. Milly, and an anonymous referee for the detailed and constructive comments. This work was supported by grants from the European Commission-funded projects ENSEMBLES (GOCE-CT-2003-505539), CARBOEUROPE IP (GOCE-CT-2003-505572), and GREENCYCLES MC-RTN (MRTN-CT-2004-512464). Computer time was provided by Commissariat à l'Énergie Atomique.

1. Gedney N, Cox PM, Betts RA, Boucher O, Huntingford C, Stott PA (2006) *Nature* 439:835–838.
2. Labat D, Godderis Y, Probst JL, Guyot JL (2004) *Adv Water Res* 27:631–642.
3. Milly PCD, Dunne KA, Vecchia AV (2005) *Nature* 438:347–350.
4. de Wit M, Stankiewicz J (2006) *Science* 311:1917–1921.
5. Oki T, Kanae S (2006) *Science* 313:1068–1072.
6. Field CB, Jackson RB, Mooney HA (1995) *Plant Cell Environ* 18:1214–1225.
7. Cowling SA, Field CB (January 11, 2003) *Global Biogeochem Cycles*, 10.1029/2002GB001915.
8. Sahin V, Hall MJ (1996) *J Hydrol* 178:293–309.
9. Costa MH, Foley JA (1997) *J Geophys Res* 102:23973–23989.
10. Jackson RB, Jobbagy EG, Avissar R, Roy SB, Barrett DJ, Cook CW, Farley KA, le Maitre DC, McCarl BA, Murray BC (2005) *Science* 310:1944–1947.
11. Foley JA, DeFries R, Asner GP, Barford C, Bonan G, Carpenter SR, Chapin FS, Coe MT, Daily GC, Gibbs HK, *et al*. (2005) *Science* 309:570–574.
12. Krinner G, Viovy N, de Noblet-Ducoudre N, Ogee J, Polcher J, Friedlingstein P, Ciais P, Sitch S, Prentice IC (February 26, 2005) *Global Biogeochem Cycles*, 10.1029/2003GB002199.
13. Chahine MT (1992) *Nature* 359:373–380.
14. Norby RJ, DeLucia EH, Gielen B, Calfapietra C, Giardina CP, King JS, Ledford J, McCarthy HR, Moore DJP, Ceulemans R, *et al*. (2005) *Proc Natl Acad Sci USA* 102:18052–18056.
15. Betts RA, Cox PM, Lee SE, Woodward FI (1997) *Nature* 387:796–799.
16. Levis S, Foley JA, Pollard D (2000) *J Clim* 13:1313–1325.
17. Costa MH, Botta A, Cardille JA (2003) *J Hydrol* 283:206–217.
18. Curtis PS, Wang XZ (1998) *Oecologia* 113:299–313.
19. Gill RA, Polley HW, Johnson HB, Anderson LJ, Maherali H, Jackson RB (2002) *Nature* 417:279–282.
20. Nie D, He H, Mo G, Kirkham MB, Kanemasu ET (1992) *Agric For Met* 61:205–217.
21. Pinter PJ, Kimball BA, Mauney JR, Hendrey GR, Lewin KF, Nagy J (1994) *Agric For Met* 70:209–230.
22. Döll P, Siebert S (April 26, 2002) *Water Resour Res*, 10.1029/2001WR000355.
23. Gordon LJ, Steffen W, Jonsson BF, Folke C, Falkenmark M, Johannessen A (2005) *Proc Natl Acad Sci USA* 102:7612–7617.
24. Milly PCD, Dunne KA (1994) *J Clim* 7:506–526.
25. Moore N, Rojstaczer S (August 16, 2002) *Geophys Res Lett*, 10.1029/2002GL014940.
26. Ducoudre NI, Laval K, Perrier A (1993) *J Clim* 6:248–273.
27. Ball J, Woodrow T, Berry J (1987) *Prog Photosynthesis* 4:221–224.
28. Verant S, Laval K, Polcher J, De Castro M (2004) *J Hydrometeorol* 5:267–285.
29. Ngo-Duc T, Laval K, Polcher J, Cazenave A (May 3, 2005) *J Geophys Res*, 10.1029/2994JD004940.
30. Ngo-Duc T, Laval K, Polcher J, Lombard A, Cazenave A (May 12, 2005) *Geophys Res Lett*, 10.1029/2006GL028205.
31. Ciais P, Reichstein M, Viovy N, Granier A, Ogee J, Allard V, Aubinet M, Buchmann N, Bernhofer C, Carrara A, *et al*. (2005) *Nature* 437:529–533.
32. Piao SL, Friedlingstein P, Ciais P, Zhou LM, Chen AP (December 9, 2006) *Geophys Res Lett*, 10.1029/2006GL028205.
33. Morales P, Sykes MT, Prentice IC, Smith P, Smith B, Bugmann H, Zierl B, Friedlingstein P, Viovy N, Sabate S, *et al*. (2005) *Global Change Biol* 11:2211–2233.
34. Mitchell TD, Jones PD (2005) *Int J Climatol* 25:693–712.
35. Rayner PJ, Scholze M, Knorr W, Kaminski T, Giering R, Widmann H (June 15, 2005) *Global Biogeochem Cycles*, 10.1029/2004GB002254.
36. Ramankutty N, Foley JA (1999) *Global Biogeochem Cycles* 13:997–1027.
37. Goldewijk KK (2001) *Global Biogeochem Cycles* 15:417–433.
38. Loveland TR, Reed BC, Brown JF, Ohlen DO, Zhu Z, Yang L, Merchant JW (2000) *Int J Remote Sens* 21:1303–1330.